A benchmark white dwarf–ultracool dwarf wide field binary

Thiago Ferreira [1,2]★ Roberto K. Saito [3] Dante Minniti,[3,4,5] Andrea Mejías,[4] Claudio Caceres [4,6]
Javier Alonso-García,[7,8] Juan Carlos Beamín [4] Leigh C. Smith,[9] Matías Gomez,[4] Philip W. Lucas [10]
and Valentin D. Ivanov[11]

[1]*Department of Astronomy, Yale University, 219 Prospect St., New Haven, CT 06511, USA*
[2]*Instituto de Astronomia, Geofísica e Ciências Atmosféricas, Universidade de São Paulo, 05508-090 São Paulo, Brazil*
[3]*Departamento de Física, Universidade Federal de Santa Catarina, Trindade 88040-900, Florianópolis, Brazil*
[4]*Instituto de Astrofísica, Facultad de Ciencias Exactas, Universidad Andres Bello, Av. Fernández Concha 700, Santiago, Chile*
[5]*Vatican Observatory, I-00120 Vatican City State, Italy*
[6]*Nu´cleo Milenio de Formacio´n Planetaria - NPF, Universidad de Valparaiso, Av. Gran Bretana 1111, Valparaiso, Chile*
[7]*Centro de Astronomía (CITEVA), Universidad de Antofagasta, 02800, Av. Angamos 601, Antofagasta, Chile*
[8]*Millennium Institute of Astrophysics, Nuncio Monseñor Sotero Sanz 100, Of. 104, Providencia, Santiago, Chile*
[9]*Institute of Astronomy, University of Cambridge, Madingley Road, Cambridge CB3 0HA, UK*
[10]*Centre for Astrophysics, University of Hertfordshire, College Lane, Hatfield AL10 9AB, UK*
[11]*European Southern Observatory, Karl-Schwarzschild-Straße 2, D-85748 Garching bei München, Germany*

ABSTRACT

We present the discovery and multiwavelength characterization of VVV J1438-6158 AB, a new field wide-binary system consisting of a $4.6^{+5.5}_{-2.4}$ Gyr and $T_{\rm eff} = 9500 \pm 125$ K DA white dwarf (WD) and a $T_{\rm eff} = 2400 \pm 50$ K M8 ultracool dwarf (UCD). The projected separation of the system is $a = 1236.73$ au (~ 13.8 arcsec), and although along the line of sight towards the Scorpius–Centaurus stellar association, VVV J1438-6158 AB is likely to be a field star, from a kinematic 6D probabilistic analysis. We estimated the physical and dynamical parameters of both components via interpolations with theoretical models and evolutionary tracks, which allowed us to retrieve a mass of 0.62 ± 0.18 $M_{\odot}$ for the WD, and a mass of 98.5 ± 6.2 $M_{\rm Jup}$ ($\sim 0.094 \pm 0.006$ $M_{\odot}$) for the UCD. The radii of the two components were also estimated at 0.01309 ± 0.0003 $R_{\odot}$ and 1.22 ± 0.05 $R_{\rm Jup}$, respectively. VVV J1438-6158 AB stands out as a benchmark system for comprehending the evolution of WDs and low-mass companions given its status as one of the most widely separated WD+UCD systems known to date, which likely indicates that both components may have evolved independently of each other, and also being characterized by a large-mass ratio ($q = 0.15 \pm 0.04$), which likely indicates a formation pathway similar to that of stellar binary systems.

Key words: brown dwarfs – stars: binaries, evolution – white dwarfs – infrared: stars.

1 INTRODUCTION

Binary systems involving a white dwarf (WD) and a companion of extremely low-mass, such as an ultracool dwarf (UCD) or brown dwarf (BD), present a unique opportunity to investigate the evolution of low-mass stars and substellar objects. The working definition and distinction between BDs ($T_{\rm eff} \leq 2200$ K), and UCDs ($T_{\rm eff} \leq 2700$ K) are based on their masses and temperatures. Both surpass the planetary threshold for deuterium burning in their cores ($\sim 14 - 16$ $M_{\rm Jup}$; Spiegel, Burrows & Milsom 2011), but BDs fall short of initiating hydrogen nuclear fusion ($\sim 80 - 85$ $M_{\rm Jup}$; Kumar 1963; Burrows et al. 2001). In the upper span of their mass spectrum ($\gtrsim 60$ $M_{\rm Jup}$), their sizes are predominantly regulated by electron-degeneracy pressure, alike WDs, while at the lower limit of this range ($\sim 14 - 20$ $M_{\rm Jup}$), their sizes are mainly determined by Coulomb pressure (Basri & Brown 2006). WDs, on the other

hand, are remnants of stars with masses in the main sequence ranging from 0.8 to 7.5 $M_{\odot}$ (Weidemann 1968; Saumon, Blouin & Tremblay 2022), composed primarily of degenerate matter, and are supported against gravitational collapse by electron-degeneracy pressure.

Significant progress has been achieved in the investigation of cataclysmic variable stars (CVs) involving stellar remnants and substellar objects (e.g. Longstaff et al. 2019; Zorotovic & Schreiber 2022, and references therein), however, many of these systems are distinguished by their close proximity, often leading to common envelope interactions and profound influence on each other component's evolution.

VVV J1438-6158 AB was discovered from the investigation of low-mass stars and free-floating planets (FFPs) towards the young Lower Centaurus–Crux stellar association (LCC; de Zeeuw et al. 1999) by Mejías et al. (2022). Differing from previously known WD+UCD/BD binaries (e.g. Farihi & Christopher 2004; Farihi, Becklin & Zuckerman 2005; Schmidt et al. 2005; Steele et al. 2009, 2013; Casewell et al. 2012; Beuermann et al. 2013; Catalán

★ E-mail: thiago.dossantos@yale.edu

Table 1. *Gaia* DR3 astrometric measurements and derived parameters for VVV J1438-6158 AB. *Note*: Component A (first row) corresponds to the WD, while component B (second row) corresponds to the UCD.

Gaia DR3 ID	α (deg)	δ (deg)	$\overline{\pi}$ (mas)	$\mu_\alpha \cos\delta$ (mas yr^{-1})	μ_δ (mas yr^{-1})	RUWE	Δ (pc)
5877522801734482432	219.624 ± 0.0387	-61.9806 ± 0.0446	11.162 ± 0.066	-14.975 ± 0.062	-31.019 ± 0.060	0.956	89.6 ± 0.5
5877522797372878208	219.628 ± 0.2409	-61.9840 ± 0.2704	11.545 ± 0.389	-14.231 ± 0.378	-29.604 ± 0.372	1.180	86.6 ± 2.9

2013; Littlefair et al. 2014; Longstaff et al. 2019), and also from the first BD discovered by the VISTA Variables in the Via Lactea (VVV) survey not belonging to a binary system (VVV BD001; Beamín et al. 2013), in terms of orbital separation, VVV J1438-6158 AB resides at the opposite end of the spectrum, exhibiting a notably loose configuration wherein both components appear to have evolved independently from one another, i.e. without exerting any discernible influence on each other's evolutionary paths. Its significance relies upon the scarcity, albeit non-absence, of systems with well-established ages similar to it. A similar WD+UCD binary system, WD0837+185, was also discovered within the Praesepe cluster (Casewell et al. 2012), however, it differs from the system reported here with its much closer projected separation of ~ 0.006 au and age of 625 Myr, which likely implies interaction, making unlikely the independent evolution of its components. As of the current writing, there are eight known WD+UCD/BD binaries, spanning a range from relative proximity between the components ($a < 100$ au; Steele et al. 2013), or exhibiting an intermediate configuration (e.g. Becklin & Zuckerman 1988; Meisner et al. 2020; French et al. 2023), to loose separations ($a > 1000$ au; e.g. Day-Jones et al. 2011; Luhman, Burgasser & Bochanski 2011; Rodriguez et al. 2011; Deacon et al. 2014).

In this paper, we present the characterization of VVV J1438-6158 AB, a new WD+UCD binary system towards the young Scorpius–Centaurus (Sco–Cen) stellar association. In Section 2, we describe the observational data used in the analysis, focusing on the multicolour photometry obtained for both components: G, BP, and RP magnitudes from *Gaia* DR3 (Gaia Collaboration 2021), $grizY$ magnitudes from DECam Plane Survey (DECaPS; Schlafly et al. 2018), and $ZYJHK_s$ magnitudes from the VVV survey (Minniti et al. 2010). In Section 3, we present the physical parameters of WD and its companion, including effective temperatures, masses, radii, surface gravities, and ages from interpolation with theoretical models. In Section 4, we briefly discuss the likelihood of membership to Sco–Cen by VVV J1438-6158 AB. A light-curve analysis of the system in the VVV-K_s pass-band is discussed in Section 5, and in Section 6, we present our conclusions, summarizing the key findings from our analysis.

2 OBSERVATIONS OF VVV J1438-6158 AB

VVV J1438-6158 AB was identified by El-Badry, Rix & Heintz (2021) as a comoving pair with a small chance alignment probability $\mathcal{R} = 3.015 \times 10^{-5}$, who classified it as a comoving pair composed of a WD and a main-sequence (MS) star. Independently, we classified the system as a field binary consisting of a WD and a UCD towards the Sco–Cen stellar association from data of the VVV survey and *Gaia* DR3. In the absence of radial velocity measurements for both components of VVV J1438-6158 AB, we cannot estimate the 3D space velocity, nor the difference, for the system. Nevertheless, the high-bound probability assumption for the system relies on $\mathcal{R} \ll 0.1$, which corresponds approximately to ≥ 90 per cent bound probability (e.g. El-Badry, Rix & Heintz 2021). Table 1 presents

the *Gaia* DR3 measurements for both components, encompassing locations, parallaxes, proper motions in equatorial components, the renormalized unit weight errors (RUWEs), and distances derived from the parallax measurements.

We adopt a distance of 89.6 ± 0.5 pc for this system based on the more accurately measured parallax value of the WD component, which has an uncertainty of 0.07 mas. Its Galactic space velocities components are $U = -0.508$, $V = 4.392$, and $W = -1.569$ km s^{-1} from Torres et al. (2019), which suggests that the system belongs to the thin disc. The tangential velocity of both components, $V_t = 4.74 \times \mu_{total} \times \Delta$, was estimated at $V_{t,WD} = 14.62 \pm 0.02$ and $V_{t,UCD} = 17.87 \pm 0.15$ km s^{-1}. The projected separation between the WD and UCD is 13.8 arcsec, which corresponds to a physical separation of ~ 1240 au at that distance, and note that the RUWE values for both components are relatively low, which indicates reliable astrometric estimations from *Gaia* (Lindegren et al. 2021), and that both components do not likely possess close stellar companions (Fitton, Tofflemire & Kraus 2022).

Although the WD companion was too faint to be detected during observations of the 2MASS survey (Two Micron All Sky Survey; Skrutskie et al. 2006), the UCD was detected (source ID 2MASS J14383082-6159022). For both components, however, near-infrared (IR) $ZYJHK_s$ photometry was obtained by the VVV survey (Minniti et al. 2010). They are situated within the overlapping region of the Galactic disc VVV tiles d014 and d015, and despite the crowded nature of the field, the optical and near-IR images suggest that they remain relatively uncontaminated (see Fig. 1).

Fig. 2 depicts the optical and near-IR colour–magnitude (CMD) and colour–colour diagrams (CCD) of the surrounding field (5 arcmin of the central location of the WD) containing the targets. In both diagrams, the two components are separated. Solar metallicity isochrones[1] (PARSEC v1.2S and COLIBRI S$_{35}$ tracks; Chen et al. 2014; Pastorelli et al. 2019) for ages of $1 - 10$ Gyr, extinctions A_V ranging from $0 - 8$ mag, shifted to the distance of the Galactic centre, ≈ 8.7 kpc (Vanhollebeke, Groenewegen & Girardi 2009), are overlaid to the CMDs and CCD. VVV J1438-6158 AB is located in a region of relatively high reddening,[2] with a measured colour excess $E(B - V)_{SFD} = 1.75 \pm 0.06$ mag, and visual extinction $A_{V,SFD} = 5.42 \pm 0.19$ mag (Schlegel, Finkbeiner & Davis 1998; Schlafly & Finkbeiner 2011), while the colour excess at the distance of the system $[E(B - V)_\Delta]$ is 0.012 ± 0.017 mag and the visual extinction also at the distance of the system ($A_{V,\Delta}$) is 0.037 ± 0.052 mag (Capitanio et al. 2017).[3]

Table 2 presents the photometric data for the WD and UCD obtained from various optical and near-IR catalogues, including the *Gaia* DR3, DECaPS, VVV, and 2MASS (Skrutskie et al. 2006). The absolute magnitudes in *Gaia*$-G$, and VVVX$-J/K_s$ bands, assuming a distance of $\Delta = 89.6$ pc for this system, are provided in the

[1] http://stev.oapd.inaf.it/cgi-bin/cmd
[2] https://irsa.ipac.caltech.edu/DUST/
[3] https://stilism.obspm.fr/
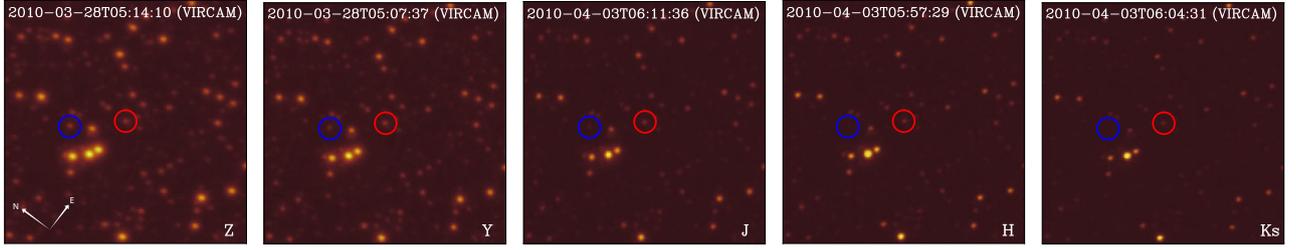
Figure 1. Near-IR finding charts from the VVV DR5 of the WD (component A; circle on the left), and its UCD companion (component B; centre of the figures) in $ZYJHK_s$ pass-bands in 2010. Despite the crowded nature of the field, the binary components are well-separated (13.8 arcsec), and visibly, the UCD is brighter than the WD at longer near-IR wavelengths. All images have the same orientation as indicated in the first panel.
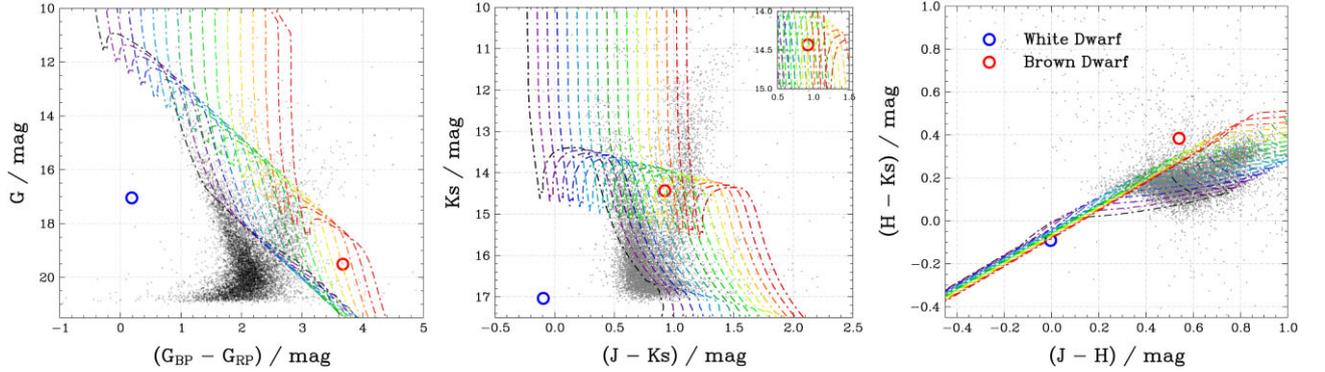
Figure 2. Optical *Gaia G* versus $BP - RP$ (first panel), near-IR VVV K_s versus $J - K_s$ CMD (second panel), and $J - H$ versus $H - K_s$ CCD (third panel) diagrams for a 5 arcmin field centred on the WD+UCD binary pair. The WD is shown with a blue circle and the UCD with a red circle. Evolutionary tracks for distinct A_V in each panel are from PARSEC v1.2S + COLIBRI S$_{35}$.

Table 2. Optical and near-IR photometry of VVV J1438-6158 AB binary.

Survey	Filter	WD (A)	UCD (B)
Gaia DR3 (Vega)	G	17.05 ± 0.01	19.51 ± 0.01
Gaia DR3 (Vega)	BP	17.12 ± 0.01	21.43 ± 0.22
Gaia DR3 (Vega)	RP	16.93 ± 0.01	17.76 ± 0.01
VVV (Vega)	J	16.94 ± 0.03	15.43 ± 0.02
VVV (Vega)	H	16.87 ± 0.03	14.87 ± 0.02
VVV (Vega)	K_s	16.89 ± 0.03	14.55 ± 0.02
2MASS (Vega)	J	–	15.38 ± 0.02
2MASS (Vega)	H	–	14.74 ± 0.03
2MASS (Vega)	K_s	–	13.93 ± 0.05
DECaPS (AB)	g	17.05 ± 0.01	23.34 ± 0.10
DECaPS (AB)	r	17.13 ± 0.01	21.47 ± 0.05
DECaPS (AB)	i	17.24 ± 0.01	18.43 ± 0.01
DECaPS (AB)	z	17.40 ± 0.01	17.25 ± 0.01
DECaPS (AB)	Y	17.49 ± 0.01	16.88 ± 0.01
Gaia DR3	M_G	12.28 ± 0.07	14.76 ± 0.07
VVVX (Vega)	M_J	12.17 ± 0.08	10.65 ± 0.07
VVVX (Vega)	M_{K_s}	12.47 ± 0.08	13.66 ± 0.07

last rows. Conservative errors were considered, primarily influenced by the measured parallax difference between both components. It is worth noting the absence of near-IR excess in the WD's colours, which suggests the absence of an additional close companion, or a circumstellar disc. Moreover, a thorough examination of the near-IR CCD diagram presented in Steele et al. (2011) (refer to their Fig. 1, which also relies on the findings of Wellhouse et al. 2005), confirms that the WD occupies a distinct position within the solitary WD region.

3 SPECTRAL ENERGY DISTRIBUTION (SED) ANALYSIS

We integrated the observed fluxes from the optical ($\lambda_{min} = 4673.24$ Å) to IR-region ($\lambda_{max} = 21376$ Å) using the Virtual Observatory Spectral Energy Distribution (SED) Analyser[4] web tool (VOSA; Bayo et al. 2008) to estimate the physical and atmospheric parameters of both components of VVV J1438-6158 AB system. Fig. 3 depicts their multifrequency SED collected from the *Gaia*, DECaPS, and VVV surveys, and Table 3 summarises the main properties of both components of VVV J1438-6158 AB binary system.

3.1 WD's characterization

In the *Gaia* EDR3 catalogue, VVV J1438-6158 A is classified as a WD with 99.47 per cent probability (Gentile Fusillo et al. 2021), and have 79.3 per cent probability of being a DA-type WD (with a predominantly hydrogen rich atmosphere; Jiménez-Esteban et al. 2023). Pure hydrogen and pure helium atmospheric models from Gentile Fusillo et al. (2021) yielded effective temperatures of $T_{eff,H/He} = 9588.61 \pm 123.51/9405.41 \pm 128.14$ K, surface gravities at $\log(g)_{H/He} = 7.98 \pm 0.04/7.89 \pm 0.04$, and masses $M_{H/He} = 0.58 \pm 0.02/0.51 \pm 0.02$ M$_\odot$.

The best-fitting to the available photometric measurements of VVV J1438-6158 A (Table 2) was obtained with the WD spectra and atmosphere model library presented in Koester (2010), yielding an effective temperature of $T_{eff} = 9500 \pm 125$ K and surface gravity

[4] http://svo2.cab.inta-csic.es/theory/vosa/
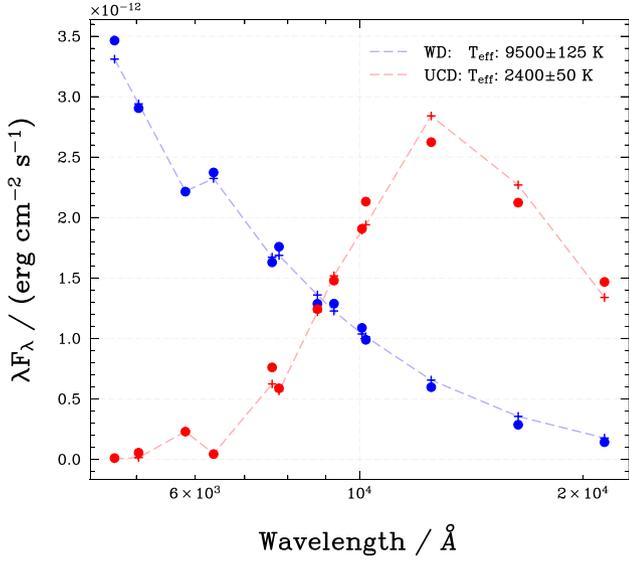
Figure 3. SED fitting of VVV J1438-6158 AB pair. The circles correspond to the observed flux for both components (red for the UCD and blue for the WD), while the dashed lines plus crosses correspond to the respective best-fitting models.

Table 3. Fundamental properties of VVV J1438-6158 AB binary retrieved with SED analysis.

	Value	Description
White Dwarf		
Sp. T.	DA	Spectral type
T_{eff} (K)	9500 ± 125	Effective temperature
$\log(g)$ (cgs)	8.00 ± 0.12	Surface gravity
L_{bol} ($L_\odot$)	$(1.257 \pm 0.005) \times 10^{-3}$	Bolometric luminosity
M ($M_\odot$)	0.62 ± 0.18	Mass (Solar units)
R ($R_\odot$)	0.01309 ± 0.0003	Radius (Solar units)
R ($R_\oplus$)	1.42 ± 0.03	Radius (Earth units)
τ (Gyr)	$0.74^{+0.09}_{-0.06}$	Cooling age
Γ (Gyr)	$4.6^{+5.5}_{-2.4}$	WD's total age
Γ' (Gyr)	$3.8^{+5.6}_{-2.5}$	Main-sequence age
M_{init} ($M_\odot$)	$1.37^{+0.63}_{-0.32}$	WD progenitor's mass
Ultracool Dwarf		
Sp. Type	M8	Spectral type
T_{eff} (K)	2400 ± 50	Effective temperature
$\log(g)$ (cgs)	5.21 ± 0.04	Surface gravity
L_{bol} ($L_\odot$)	$(5.60 \pm 0.02) \times 10^{-4}$	Bolometric luminosity
M ($M_\odot$)	0.094 ± 0.006	Mass (Solar units)
M (M_{Jup})	98.47 ± 6.28	Mass (Jupiter units)
R (R_{Jup})	1.22 ± 0.05	Radius (Jupiter units)
R ($R_\odot$)	0.1253 ± 0.005	Radius (Solar units)
ρ (g cm^{-3})	67.25 ± 9.31	Density
P_{orb} (yr)	$(141.85 \pm 4.52) \times 10^3$	Orbital period (years)
Ω (au)	1236.73	Projected separation
$\mathcal{R}$	3.015×10^{-5}	Chance alignment prob.

$\log(g) = 8.00 \pm 0.12$, with $\chi^2_\nu = 1.38$ (11 free parameters). The bolometric luminosity for the adopted distance is $L_{bol} = (1.257 \pm 0.005) \times 10^{-3}$ $L_\odot$, and applying the Stefan–Boltzmann law led to an estimation of the object's radius as $R = 0.01309 \pm 0.0003$ $R_\odot$. From the best-fitting surface gravity and estimated radius, the WD's mass was determined as $M = 0.63 \pm 0.18$ $M_\odot$. Within their uncertainties, these WD parameters appear to be similar to what

Table 4. VVV near-IR photometry of VVV J1438-6158 AB pair. The full version of this table is available in the supplementary material, where VVV ID 11846281028924 stands for the WD companion, and VVV ID 11846281000738 stands for the UCD companion.

VVV ID	MJD	Filter	Magnitude	σ /mag
11846281028924	55260.349798	K_s	16.781	0.1271
11846281028924	55260.350439	K_s	16.933	0.1365
11846281028924	55283.213633	Y	16.821	0.0148
11846281028924	55283.215090	Y	16.818	0.0159
11846281028924	55283.218185	Z	16.826	0.0128
11846281028924	55283.219530	Z	16.844	0.0138
11846281028924	55288.357982	H	16.854	0.0354
11846281028924	55288.359438	H	16.865	0.0296
11846281028924	55288.362746	K_s	17.007	0.0886
...	...	...	...	
11846281000738	55260.349798	K_s	14.528	0.0191
11846281000738	55260.350439	K_s	14.583	0.0311
11846281000738	55283.213633	Y	16.043	0.0081
11846281000738	55283.215090	Y	16.052	0.0079
11846281000738	55283.218185	Z	16.955	0.0192
11846281000738	55283.219530	Z	16.936	0.0169
11846281000738	55288.357982	H	14.877	0.0126
11846281000738	55288.359438	H	14.872	0.0083
11846281000738	55288.362746	K_s	14.551	0.0357
...	...	...	...	

has been derived for similar objects (e.g. Chandrasekhar 1935; Schwarzschild 1958; Landau & Lifshitz 1969). Alternatively, a direct blackbody fit resulted in $T_{eff,BB} = 9900 \pm 25$ K, and $L_{bol,BB} = 1.257 \times 10^{-3} \pm 1.6 \times 10^{-6}$ $L_\odot$.

3.1.1 WD's age and progenitor mass

To estimate the age of VVV J1438-6158 A, we used the wdwarfdate software (Kiman et al. 2022), which adopts a Bayesian approach for thick hydrogen (DA) and non-DA layer, taking into account the remnant's effective temperature and surface gravity. This approach allowed us to estimate the final mass of the WD and the initial mass of its progenitor. For a DA WD, the main-sequence age and mass were derived as $\Gamma_{DA} = 3.88^{+5.57}_{-2.51}$ Gyr and $M_{init,DA} = 1.37^{+0.63}_{-0.32}$ $M_\odot$, respectively, from an initial-final mass relation model of Cummings et al. (2018), a cooling model from Bédard et al. (2020), and evolutionary tracks from Choi et al. (2016) and Dotter (2016).

Fig. 4 depicts the optical G versus $G_{BP} - G_{RP}$ CMD for nearby objects presented in the *Gaia* catalogue, and the positioning of VVV J1438-6158 A in such a diagram. Overlaid to the CMD are indicated evolutionary cooling tracks[5] for pure-hydrogen DA- and pure-helium DB-type WDs with $\log(g) = 7.5 - 9.0$ from Holberg & Bergeron (2006) and Bédard et al. (2020).

With WDWARFDATE we obtained a cooling age of $\tau_{DA} = 0.74^{+0.09}_{-0.06}$ Gyr, resulting in a total age of $\Gamma'_{DA} = 4.6^{+5.44}_{-2.43}$ Gyr for VVV J1438-6158 A. The derived final WD's mass using this approach was $M_{DA} = 0.61^{+0.05}_{-0.04}$ $M_\odot$, which is consistent within its uncertainties with previous findings. Furthermore, the results obtained from the SED analysis agree with this estimate, indicating that the WD likely belongs to an older population of stars, formed from a relatively low-mass progenitor, and has undergone a rapid cooling process since its formation (e.g. Segretain & Chabrier 1993; Chabrier et al. 2000; Isern et al. 2000). For the non-DA WD case, we obtained

---

[5] https://www.astro.umontreal.ca/~bergeron/CoolingModels/
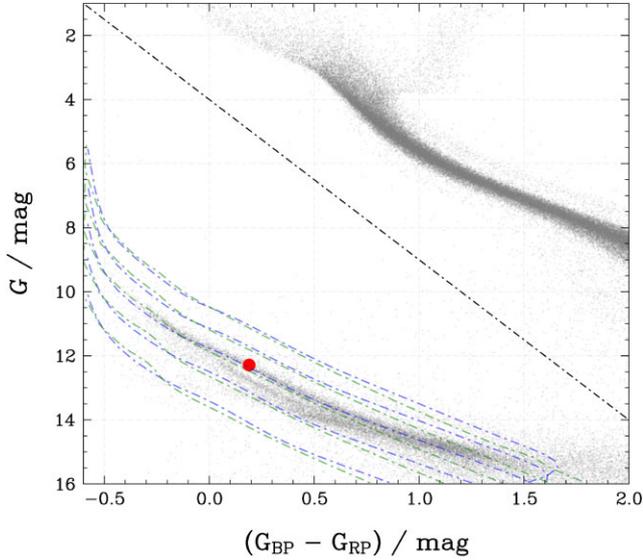
Figure 4. Optical *Gaia* absolute *G* versus $BP - RP$ CMD diagram for approximately 370.000 nearby ($\overline{\pi} < 100^{-1}$ mas) sources with high-significance parallax ($\overline{\pi}/\sigma_{\overline{\pi}} > 100$; grey-coloured background). VVV J1438-6158 A is indicated as the red dot. The blue and green dashed lines indicate evolutionary cooling tracks for DA-type (blue) and DB-type (green) WD stars with surface gravity ranging from $\log(g) = 7.0$ (top) to $\log(g) = 9.0$ (bottom; $\delta \log(g) = 0.5$).

similar values for the aforementioned parameters: $\Gamma_{nDA} = 4.36^{+5.54}_{-2.88}$ Gyr, $M_{init,nDA} = 1.3^{+0.6}_{-0.3}$ M$_\odot$, $\tau_{nDA} = 0.79^{+0.09}_{-0.07}$ Gyr, $\Gamma'_{nDA} = 5.17^{+5.48}_{-2.83}$ Gyr, and $M_{nDA} = 0.60^{+0.05}_{-0.04}$ M$_\odot$.

3.2 UCD's characterization

From the available photometric measurements of VVV J1438-6158 B (Table 2), the best-fitting was obtained with the AMES-DUSTY model (Chabrier et al. 2000; Allard et al. 2001), yielding an effective temperature of $T_{eff} = 2400 \pm 50$ K. For the system's distance, its bolometric luminosity was estimated as $L_{bol} = (5.60 \pm 0.02) \times 10^{-4}$ L$_\odot$, and applying Stefan–Boltzmann's law, VVV J1438-6158 B radius was estimated as $R = 1.22 \pm 0.05$ R$_{Jup}$. Within its uncertainties, and since we know precisely the distance of the object, those values are consistent with objects of its kind (e.g. Hayashi & Nakano 1963; Kirkpatrick et al. 1999; Burrows et al. 2001; Luhman 2012). The UCD's age is unknown, especially due to the degeneracy in the mass-age relationship for substellar objects, therefore, assuming that VVV J1438-6158 B was formed at the same time as its companion, VVV J1438-6158 A ($\Gamma = 4.6^{+5.5}_{-2.4}$ Gyr), the mass of the companion was estimated to be $M_{UCD} = 0.094 \pm 0.006$ M$_\odot$ ($= 98.5 \pm 6.3$ M$_{Jup}$), and its surface gravity was consequently estimated at $\log(g)[cgs] = 5.21 \pm 0.04$, suggesting an L/M dwarf nature (Reid & Hawley 2005; Pecaut & Mamajek 2013; Wang et al. 2022). Moreover, we estimated the spectral type of VVV J1438-6158 B as M8 from the empirical stellar spectra library of Kesseli et al. (2017) within VOSA's framework.

While we designate VVV J1438-6158 B as an UCD, we observe that its mass falls 2σ within the hydrogen burning main-sequence edge mass (HBBM) of $0.075 - 0.092$ M$_\odot$ ($\sim 78.5 - 96.3$ M$_{Jup}$; Chabrier & Baraffe 1997; Burrows et al. 2001; Auddy, Basu & Valluri 2016), in similarity to other known low-mass BDs at similar effective temperatures (e.g. Teide 1; $M = 55 \pm 15$ M$_{Jup}$ and $T_{eff} = 2.584 \pm 150$ K; Leech et al. 2000). Spectroscopic observa-
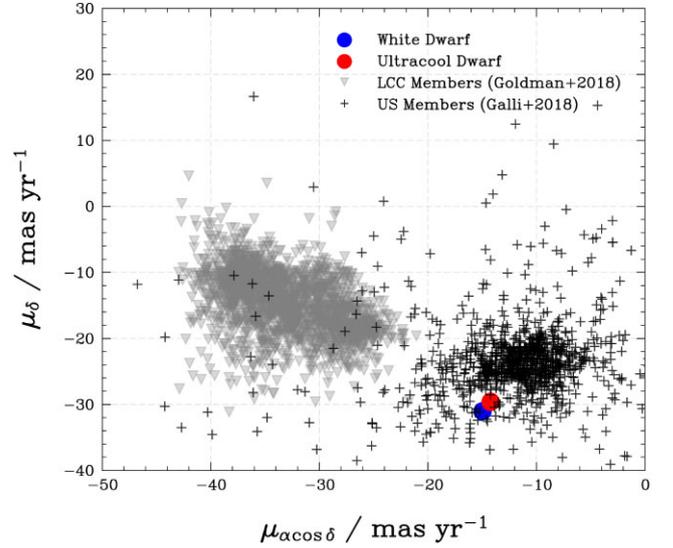
Figure 5. Proper motion distribution of LCC (grey triangles; Goldman et al. 2018) and US (black crosses; Galli, Joncour & Moraux 2018) members. The components of VVV J1438-6158 AB are depicted as blue (WD) and red (UCD) circles.

tions of VVV J1438-6158 B make itself necessary for its accurate characterization and classification.

Using Kepler's third law, by considering the masses of the WD and UCD along with their projected separation and face-on orientation, we estimated a minimum orbital period of the VVV J1438-6158 AB system as 141 ± 4 Kyr. Despite the lengthy orbital period, the system is expected to remain gravitationally bound, with a comparison with fig. 7 of Mužić et al. (2012) – stating empirical limits for the stability of a sample of binary systems – which in turn is based on Burgasser, Sheppard & Luhman (2013), supporting such a conclusion.

4 ON THE MEMBERSHIP LIKELIHOOD OF VVV J1438-6158 AB TO THE SCO–CEN ASSOCIATION

To assess the likelihood of VVV J1438-6158 AB pair being a member of the Sco–Cen stellar association, we used the BANYAN Σ algorithm based on a 6D XYZUVW kinematic analysis (Gagné et al. 2018), applying both to the LCC stellar association, the Upper Centaurus–Lupus (UCL), and Upper Scorpius (US); branches within the Sco–Cen group. This analysis indicates a null probability for the system to belong to the LCC group or any substructures within it (see Fig. 5). This conclusion is also supported by the fact that the inferred ages of the WD component (as shown in Table 3) do not align with the ages typically associated with the LCC stellar association; previous studies, for instance, by Goldman et al. (2018) and Pecaut & Mamajek (2016) suggest ages of 10 and 17 Myr, respectively.

Unlike massive stars that evolve into WDs within a few million years, the formation of a WD from relatively low-mass star progenitors generally requires a significant amount of time for a star to exhaust its nuclear fuel, shed its outer layers, and gradually cool down (Kippenhahn, Weigert & Weiss 2013). This process typically takes billions of years, making it improbable for a WD like VVV J1438-6158 A to have an age as young as 17 Myr. This inconsistency between the estimated ages and the established age range adds to evidence that contradicts VVV J1438-6158 AB's association with the LCC, supporting that the system is likely to be a field object.
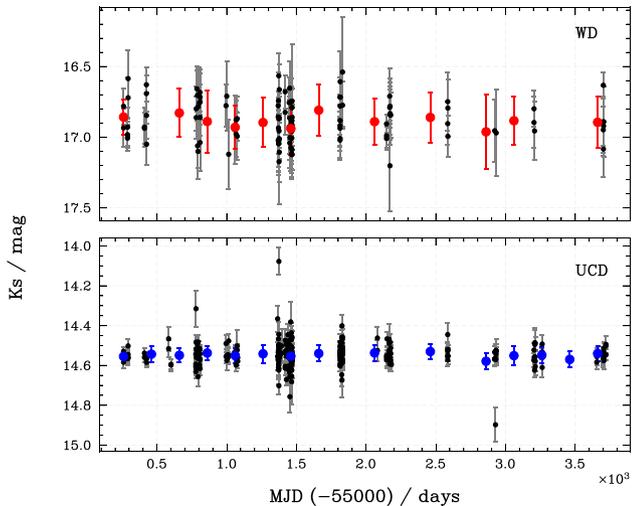
Figure 6. Observed K_s−band near-IR light curves for the WD (top panel) and UCD companions (bottom panel) spanning 10 yr. The red dots depict the moving averages for 500 d of steps.

5 NEAR-IR VVV LIGHT CURVES

Both targets are situated in the overlapping areas of two VVV tiles (d014, centred at $l = 314.40°$, $b = −1.64974°$, and d015, centred at $l = 315.83°$, $b = −1.64972°$), yielding almost twice as many observations concerning single-tile objects. However, in some of these images, the targets are too close to the edge, rendering impossible photometric measurements. Consequently, the final K_s band light curves consist of 115 photometric data points for the WD (46 in d014 and 69 in d015), and 285 for the UCD companion (104 in d014 and 181 in d015), respectively. In addition, there are 7 measurements in the $Z−$ and $Y−$bands for both components, plus 11 in the $J−$band and 6/5 measurements in the $H−$band for both the WD/BD (see Table 4). The VVV $K_s−$filter light curves for the UCD and WD are presented in Fig. 6.

We examined periodic patterns in the VVV $K_s−$band light curves of both the companions of the VVV J1438-6158 AB pair within a range of 0.1 d up to half of the full baseline with the generalized Lomb–Scargle (GLS; Zechmeister & Kürster 2009), Box-fitting Least Squares (BLS; Kovács, Zucker & Mazeh 2002), Phase Dispersion Minimisation (PDM; Stellingwerf 1978), and Multi-Harmonic Analysis of Variance (MHAOV; Schwarzenberg-Czerny 1996) algorithms through the ASTROBASE software (Bhatti et al. 2021).

VVV J1438-6158 A displays variability with a median absolute variation of 0.08 mag and root-mean square of 0.13 mag at a mean magnitude of 16.88 mag. The period search analysis reveals a prominent modulation at 0.112 d ($\sim$161.2 min) with the GLS method, which could be associated with periodic patterns caused by surface magnetic variations on the WD that become visible as it rotates, e.g. Kilic et al. (2015, 2021) and Williams, Hermes & Vanderbosch (2022). The other period-search algorithms yielded similar periods of 0.126 and 0.109 d for the PDM and BLS algorithms, while for the MHAOV a prominent 2.076-d period was found. Given the relatively noisy nature of the resulting periodograms (see Appendix A), further investigation is needed to unveil the nature of these modulations. For VVV J1438-6158 B, slight variability was noticed in the $K_s−$band, suggesting two potential modulation periods: 1.288 d with the LS method and 1.729 d with the PDM method. None of these appears

significant given the noisy nature of the resulting periodogram (see Appendix A) and no clear sine-like variations at these periods. The UCD phase diagram recovered with MHAOV at a period of 7.73 d does not exhibit any discernible temporal variation, while applying the BLS algorithm, a modulation period of $P_{BLS,UCD} = 0.111$ d was recovered, albeit also with low-significance due to inherent noise in the periodogram. These observed modulations might be influenced by various factors, such as errors in measurements or issues with the measuring instruments, resulting in stochastic fluctuations in the data. We also note the possibility of false periods in the periodogram, potentially arising from systematic effects introduced during the data windowing process, which could involve hidden periods or non-stationary behaviour. Further investigation is also needed to unveil the nature of these modulations.

6 DISCUSSION AND CONCLUSIONS

We present the characterization of VVV J1438-6158 AB, a wide-binary system consisting of a WD and a UCD first discovered with VVV/VVVX data analysis during searches for companions to UCDs, BDs, and FFPs towards the Sco–Cen/LCC stellar association El-Badry, Rix & Heintz (2021) and independently by Mejías et al. (2022). The SED analysis of this system has been conducted from data of the *Gaia* DR3, VVV, and DECaPS survey within VOSA, to derive the physical, atmospheric, and dynamical parameters of both components. Space velocities demonstrate that the system belongs to the thin disc and is gravitationally bounded from the considerably small chance alignment probability. The DA-type WD has an effective temperature of 9500 ± 125 K, a surface gravity (cgs) of 8.00 ± 0.12, a mass of 0.62 ± 0.18 M$_\odot$, and a radius of 0.01309 ± 0.0003 R$_\odot$. The M8-type UCD, on the other hand, have an effective temperature of 2400 ± 50 K, surface gravity (cgs) of 5.20 ± 0.04, mass of 98.5 ± 6.2 M$_{Jup}$, and radius of 1.22 ± 0.05 R$_{Jup}$. These parameters are consistent with the expected characteristics of objects of their respective kinds. Spectroscopic confirmation for both members of the VVV J1438-6158 AB pair is encouraged and necessary, especially to accurately determine the spectral type of VVV J1438-6158 B beyond its photometric classification, and to assess its precise age.

VVV J1438-6158 AB stands out as a benchmark system for comprehending the evolution of WDs and their low-mass companion objects given several notable features, along with the scarcity of such reported binary types. Considering the WD's nominal mass to present 0.62 M$_\odot$, the mass ratio ($q \equiv M_{UCD}/M_{WD}$) of VVV J1438-6158 AB can be estimated as 0.15 ± 0.04, which suggests a binary-like formation scenario for this system, i.e. the two objects form independently, and their masses might not be closely related (Chabrier et al. 2014; Bowler, Blunt & Nielsen 2020). The co-natal status of the pair, as well as for other WD+UCD/MS and low-mass double binaries – both wide and close – contingent upon their gravitational binding and co-mobility, remains a subject of ongoing debate and will be investigated in a future study. Nelson et al. (2021), for instance, demonstrated that $\sim$ 73 per cent of the far ($2 \times 10^5 − 10^7$ au; 31 pairs) co-moving MS+MS binaries are co-natal, which is inline with theoretical predictions from Kamdar et al. (2019). The total age of VVV J1438-6158 A was estimated at $4.6^{+5.5}_{-2.4}$ Gyr (cooling age of $0.73^{+0.09}_{0.06}$ Gyr), and given the long orbital period of the system (141.8 ± 4.5 Kyr) plus loose separation ($\sim$ 1236.73 au), it indicates a detached coexistence, with minimal perturbations or interchanges, inviting further scrutiny into the intricate interplay of forces that governs the evolution of WD+UCD/BD/MS evolution.

ACKNOWLEDGEMENTS

DATA AVAILABILITY

The data used in this project are public and can be accessed/retrieved through the VISTA Science Archive (http://horus.roe.ac.uk/vsa/index.html), and the Virtual Observatory SED Analyser (http://svo2.cab.inta-csic.es/theory/vosa/index.php).

REFERENCES

Allard F., Hauschildt P. H., Alexander D. R., Tamanai A., Schweitzer A., 2001, ApJ, 556, 357
Auddy S., Basu S., Valluri S. R., 2016, AdAst, 2016, 574327
Basri G., Brown M. E., 2006, AREPS, 34, 193
Bayo A., Rodrigo C., Barrado Y Navascués D., Solano E., Gutiérrez R., Morales-Calderón M., Allard F., 2008, A&A, 492, 277
Beamín J. C. et al., 2013, A&A, 557, L8
Becklin E. E., Zuckerman B., 1988, Natur, 336, 656
Bédard A., Bergeron P., Brassard P., Fontaine G., 2020, ApJ, 901, 93
Beuermann K. et al., 2013, A&A, 558, A96
Bhatti W., Bouma L., Joshua, Mchris42, Price-Whelan A., John, 2021, Zenodo v0.5.3
Bowler B. P., Blunt S. C., Nielsen E. L., 2020, AJ, 159, 63
Burgasser A. J., Sheppard S. S., Luhman K. L., 2013, ApJ, 772, 129
Burrows A., Hubbard W. B., Lunine J. I., Liebert J., 2001, RvMP, 73, 719
Capitanio L., Lallement R., Vergely J. L., Elyajouri M., Monreal-Ibero A., 2017, A&A, 606, A65
Casewell S. L. et al., 2012, ApJ, 759, L34
Catalán S., 2013, MmSAI, 84, 1027
Chabrier G., Baraffe I., 1997, A&A, 327, 1039
Chabrier G., Baraffe I., Allard F., Hauschildt P., 2000, ApJ, 542, 464
Chabrier G., Brassard P., Fontaine G., Saumon D., 2000, ApJ, 543, 216
Chabrier G., Johansen A., Janson M., Rafikov R., 2014, Beuther H., Klessen R. S., Dullemond C. P., Henning T., eds. Protostars and Planets VI, Univ. Arizona Press, Tucson, p.619
Chandrasekhar S., 1935, MNRAS, 95, 207
Chen Y., Girardi L., Bressan A., Marigo P., Barbieri M., Kong X., 2014, MNRAS, 444, 2525
Choi J., Dotter A., Conroy C., Cantiello M., Paxton B., Johnson B. D., 2016, ApJ, 823, 102
Cummings J. D., Kalirai J. S., Tremblay P.-E., Ramirez-Ruiz E., Choi J., 2018, ApJ, 866, 21
Day-Jones A. C. et al., 2011, MNRAS, 410, 705
de Zeeuw P. T., Hoogerwerf R., de Bruijne J. H. J., Brown A. G. A., Blaauw A., 1999, AJ, 117, 354
Deacon N. R. et al., 2014, ApJ, 792, 119
Dotter A., 2016, ApJS, 222, 8
El-Badry K., Rix H.-W., Heintz T. M., 2021, MNRAS, 506, 2269
Farihi J., Christopher M., 2004, AJ, 128, 1868
Farihi J., Becklin E. E., Zuckerman B., 2005, ApJS, 161, 394
Fitton S., Tofflemire B. M., Kraus A. L., 2022, RNAAS, 6, 18
French J. R., Casewell S. L., Dupuy T. J., Debes J. H., Manjavacas E., Martin E. C., Xu S., 2023, MNRAS, 519, 5008
Gagné J. et al., 2018, ApJ, 856, 23
Gaia Collaboration 2021, A&A, 649, A1
Galli P. A. B., Joncour I., Moraux E., 2018, MNRAS, 477, L50
Gentile Fusillo N. P. et al., 2021, MNRAS, 508, 3877
Goldman B., Röser S., Schilbach E., Moór A. C., Henning T., 2018, ApJ, 868, 32
Hayashi C., Nakano T., 1963, PThPh, 30, 460
Holberg J. B., Bergeron P., 2006, AJ, 132, 1221
Isern J., García-Berro E., Hernanz M., Chabrier G., 2000, ApJ, 528, 397
Jiménez-Esteban F. M., Torres S., Rebassa-Mansergas A., Cruz P., Murillo-Ojeda R., Solano E., Rodrigo C., Camisassa M. E., 2023, MNRAS, 518, 5106
Kamdar H., Conroy C., Ting Y.-S., Bonaca A., Johnson B., Cargile P., 2019, ApJ, 884, 173
Kesseli A. Y., West A. A., Veyette M., Harrison B., Feldman D., Bochanski J. J., 2017, ApJS, 230, 16
Kilic M. et al., 2015, ApJ, 814, L31
Kilic M., Kosakowski A., Moss A. G., Bergeron P., Conly A. A., 2021, ApJ, 923, L6
Kiman R., Xu S., Faherty J. K., Gagné J., Angus R., Brandt T. D., Casewell S. L., Cruz K. , 2022, AJ, 164, 62
Kippenhahn R., Weigert A., Weiss A., 2013, Stellar Structure and Evolution
Kirkpatrick J. D. et al., 1999, ApJ, 519, 802
Koester D., 2010, MmSAI, 81, 921
Kovács G., Zucker S., Mazeh T., 2002, A&A, 391, 369
Kumar S. S., 1963, ApJ, 137, 1121
Landau L. D., Lifshitz E. M., 1969, Statistical Physics, Pt. 1
Leech K. et al., 2000, ASPC, 212, 82
Lindegren L. et al., 2021, A&A, 649, A2
Littlefair S. P. et al., 2014, MNRAS, 445, 2106
Longstaff E. S., Casewell S. L., Wynn G. A., Page K. L., Williams P. K. G., Braker I., Maxted P. F. L., 2019, MNRAS, 484, 2566
Luhman K. L., 2012, ARA&A, 50, 65
Luhman K. L., Burgasser A. J., Bochanski J. J., 2011, ApJ, 730, L9
Meisner A. M. et al., 2020, ApJ, 899, 123
Mejías A., Soto P., Minniti D., Cáceres C., Gómez M., 2022, cosp, 44, 591
Minniti D. et al., 2010, NewA, 15, 433
Mužić K. et al., 2012, AJ, 144, 180
Nelson T., Ting Y.-S., Hawkins K., Ji A., Kamdar H., El-Badry K., 2021, ApJ, 921, 118
Pastorelli G. et al., 2019, MNRAS, 485, 5666
Pecaut M. J., Mamajek E. E., 2013, ApJS, 208, 9
Pecaut M. J., Mamajek E. E., 2016, MNRAS, 461, 794
Reid I. N., Hawley S. L., 2005, New Light on Dark Stars Red Dwarfs, Low-Mass Stars, Brown Stars, Praxis Publishing Ltd, Singapore
Rodriguez D. R., Zuckerman B., Melis C., Song I., 2011, ApJ, 732, L29
Saumon D., Blouin S., Tremblay P.-E., 2022, PhR, 988, 1
Schlafly E. F., Finkbeiner D. P., 2011, ApJ, 737, 103
Schlafly E. F. et al., 2018, ApJS, 234, 39
Schlegel D. J., Finkbeiner D. P., Davis M., 1998, ApJ, 500, 525
Schmidt G. D., Szkody P., Silvestri N. M., Cushing M. C., Liebert J., Smith P. S., 2005, ApJ, 630, L173
Schwarzenberg-Czerny A., 1996, ApJ, 460, L107
Schwarzschild M., 1958, Structure and Evolution of the Stars
Segretain L., Chabrier G., 1993, A&A, 271, L13
Skrutskie M. F. et al., 2006, AJ, 131, 1163
Spiegel D. S., Burrows A., Milsom J. A., 2011, ApJ, 727, 57

Steele P. R., Burleigh M. R., Farihi J., Gänsicke B. T., Jameson R. F., Dobbie P. D., Barstow M. A., 2009, A&A, 500, 1207

Steele P. R., Burleigh M. R., Dobbie P. D., Jameson R. F., Barstow M. A., Satterthwaite R. P., 2011, MNRAS, 416, 2768

Steele P. R. et al., 2013, MNRAS, 429, 3492

Stellingwerf R. F., 1978, ApJ, 224, 953

Torres S., Cantero C., Rebassa-Mansergas A., Skorobogatov G., Jiménez-Esteban F. M., Solano E., 2019, MNRAS, 485, 5573

Vanhollebeke E., Groenewegen M. A. T., Girardi L., 2009, A&A, 498, 95

Wang Y.-F. et al., 2022, A&A, 660, A38

Weidemann V., 1968, ARA&A, 6, 351

Wellhouse J. W., Hoard D. W., Howell S. B., Wachter S., Esin A. A., 2005, PASP, 117, 1378

Williams K. A., Hermes J. J., Vanderbosch Z. P., 2022, AJ, 164, 131

Zechmeister M., Kürster M., 2009, A&A, 496, 577

Zorotovic M., Schreiber M., 2022, MNRAS, 513, 3587

SUPPORTING INFORMATION

Supplementary data are available at *MNRAS* online.

suppl_data

Please note: Oxford University Press is not responsible for the content or functionality of any supporting materials supplied by the authors. Any queries (other than missing material) should be directed to the corresponding author for the article.

APPENDIX A: PERIODOGRAMS AND SPECTRAL WINDOW FUNCTION FOR VVV J1438-6158 AB SYSTEM
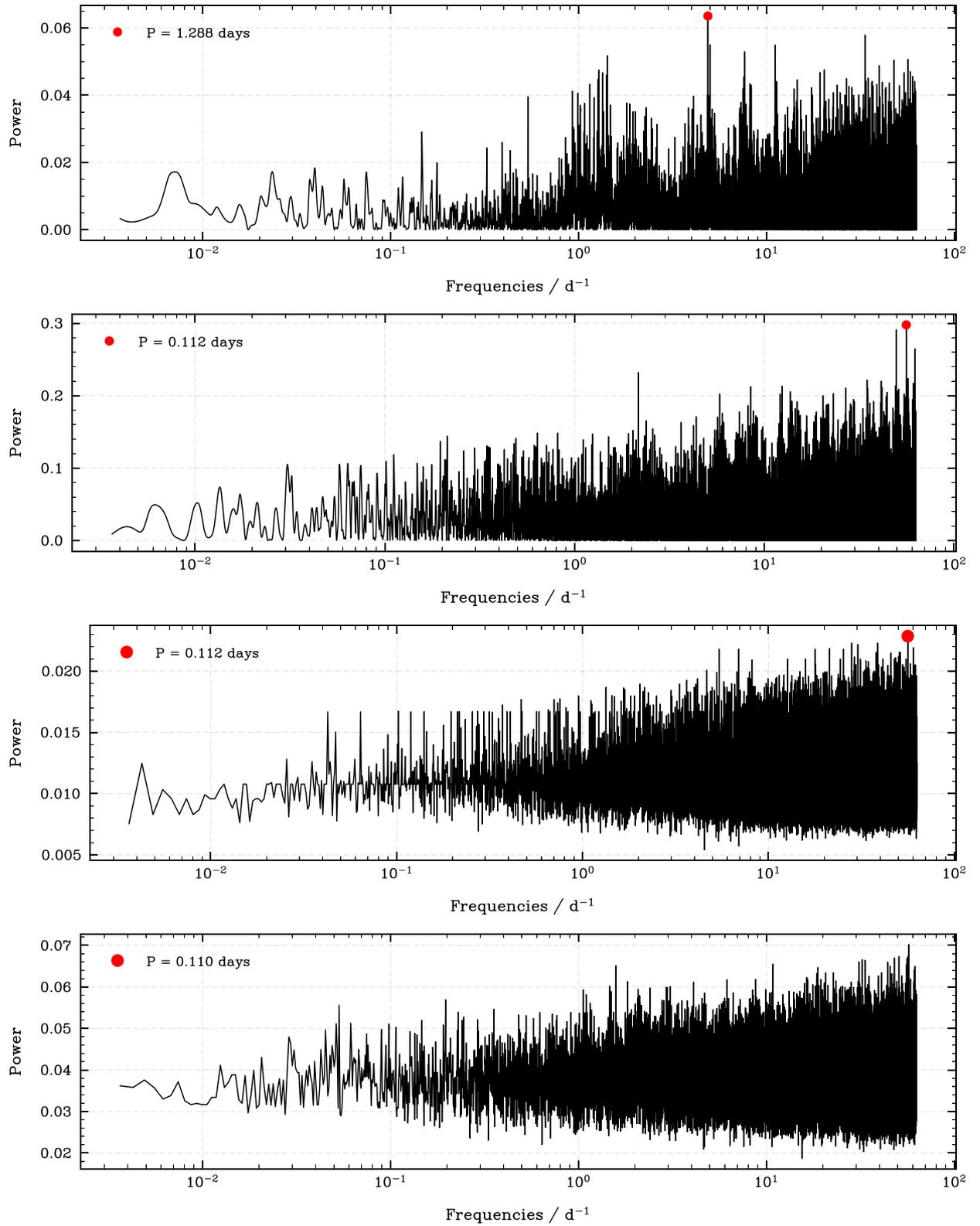
Figure A1. Lomb-Scargle (first and second panels) and Box Least-Squares (third and fourth panels) periodograms of the VVV K_s time-series of the VVV J1438-6158 B and VVV J1438-6158 A, respectively.
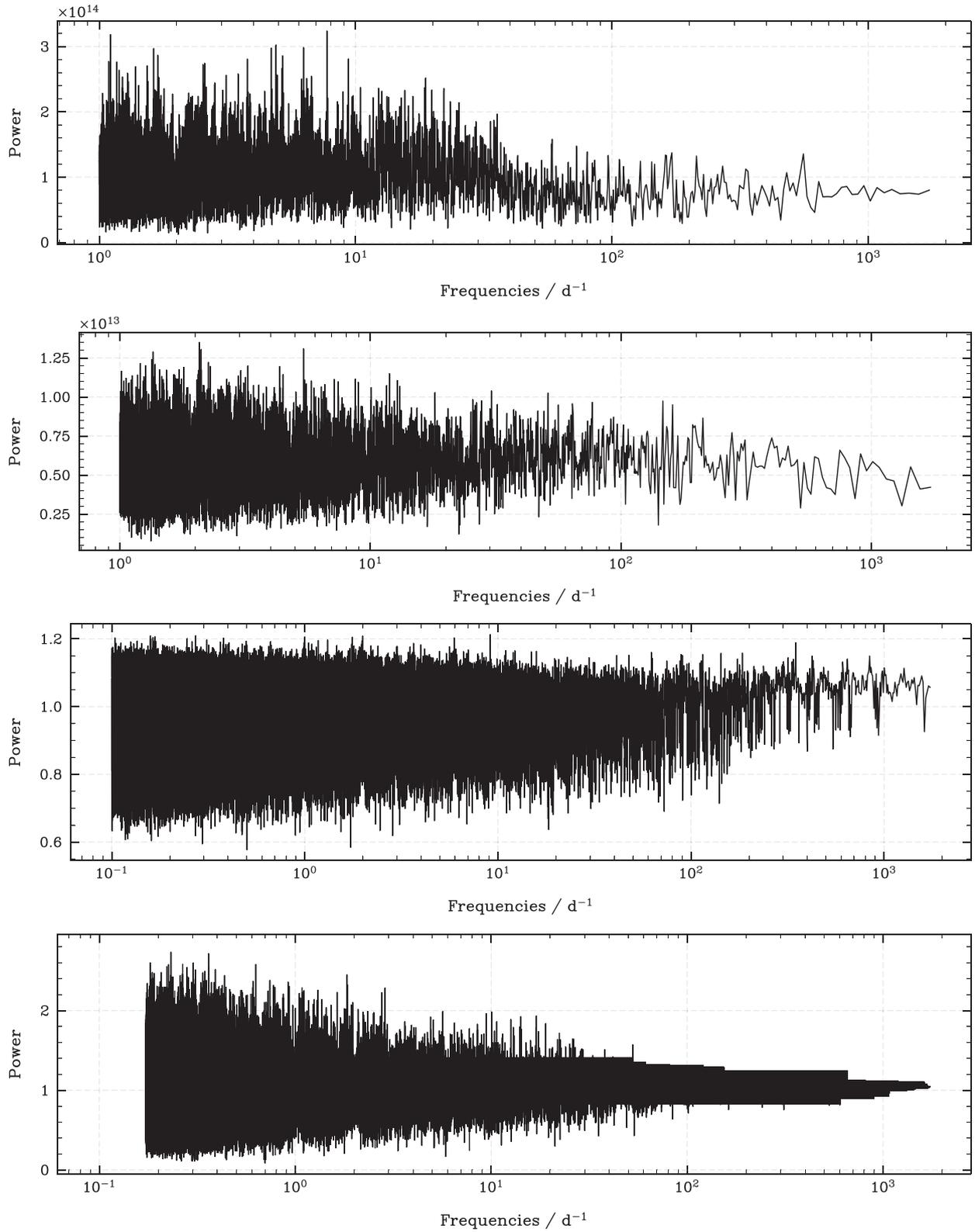
Figure A2. Multi-Harmonic Analysis of Variance (first and second panels) and Phase Dispersion Minimisation (third and fourth panels) periodograms of the VVV K_s time-series of the VVV J1438-6158 B and VVV J1438-6158 A, respectively.
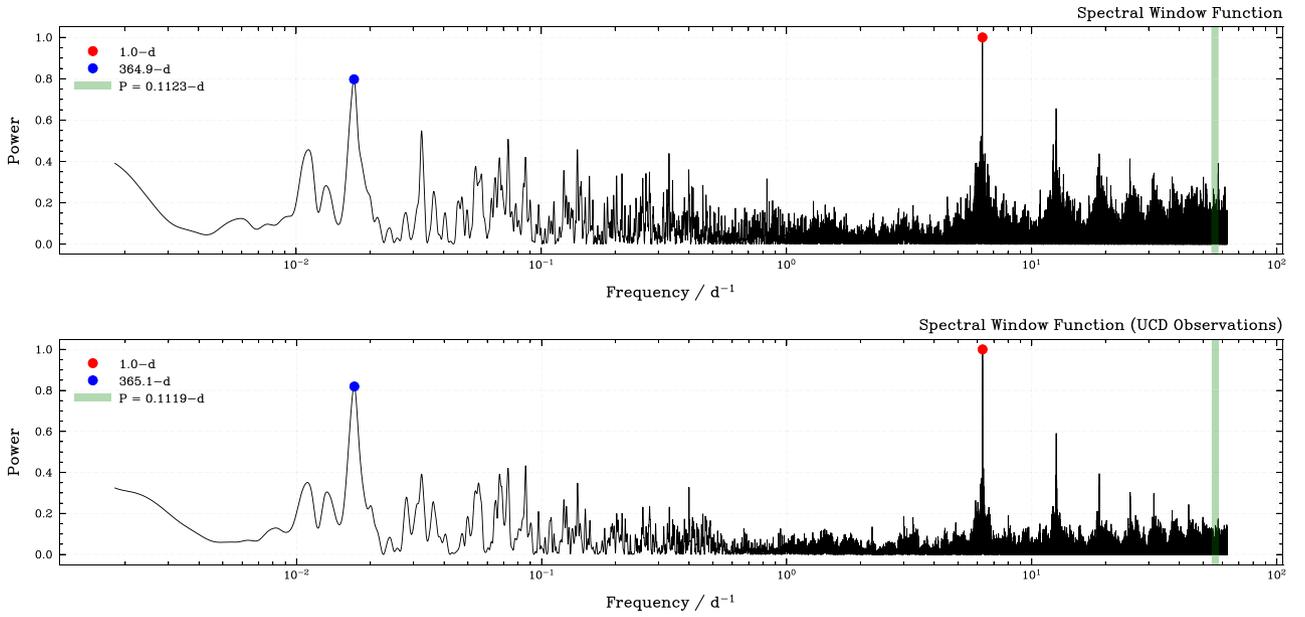
Figure A3. Spectral Window Function for VVV J1438-6158 B and VVV J1438-6158 A observations, respectively. The green vertical line marks the prominent modulation period found with the LS and BLS for both the WD and the UCD components.

This paper has been typeset from a TEX/LATEX file prepared by the author.